Sensors and Actuators A 280 (2018) 92–98

Contents lists available at ScienceDirect

Sensors and Actuators A: Physical

journal homepage: www.elsevier.com/locate/sna

Fabric-infused array of reduced graphene oxide sensors for mapping of skin temperatures

Yiqian Jin[a], Eric P. Boon[a], Linh T. Le[b], Woo Lee[a,*]

[a] Department of Chemical Engineering and Materials Science, Stevens Institute of Technology, 1 Castle Point Terrace, Hoboken, 07030, USA
[b] FlexTraPower, 175 Varick Street, New York, 10014, USA

ARTICLE INFO

Article history:
Received 20 March 2018
Received in revised form 17 May 2018
Accepted 23 June 2018
Available online 25 June 2018

Keywords:
Reduced graphene oxide
Wearable temperature sensors
Fabric-infused sensor array
Thermal imaging of skin
Smart health

ABSTRACT

We report a textile-infused sensor array, utilizing reduced graphene oxide (rGO) as a uniquely conformal negative temperature coefficient (NTC) material, for spatiotemporal mapping of skin temperatures. Nylon filaments were coated with rGO and stitched along with Ag conductive threads into a polyester fabric to create the array of individually addressable 6 × 6 NTC sensing elements. The temperature-mapping attribute of the sensor array was evaluated in comparison to infrared imaging. The rGO film remained mechanically and electrically stable upon stretching (<4% strain) and bending (<34°) of the filaments, demonstrating its conformal nature. These results suggest the intriguing possibility of thermally mapping topographically complex skin surfaces in a non-invasive, wearable, and cost effective manner.

1. Introduction

Body temperature is a vital physiological signal of our health, as humans have evolved to maintain a homeostatic core temperature of ~37 °C. Skin temperature variations, in both temporal and spatial aspects, can be measured to infer and monitor the state of our pathophysiological developments. For example, cardiovascular diseases can weaken blood circulation, thus lowering skin temperatures of ankles and toes [1–3]. In another example, a plantar temperature rise has proven to be a measurable indicator of diabetic foot ulceration [4–7]. Also, for more intriguing possibilities, emotional feelings have been correlated to topographical changes in skin temperature – happiness making the whole body warmer whereas sadness resulting in cooler arms and legs [8]. These findings suggest the enormous significance of being able to conveniently and comfortably map skin temperatures using wearable technology.

Herein we report a textile-infused sensor array for spatiotemporal mapping of skin temperatures. The wearable textile format provides: (1) intimate, conformal, and comfortable contact with topographically complex skin surfaces due to its good flexibility, stretchability, and breathability [9–12] and (2) non-invasive real-time monitoring of skin temperatures that cannot be accessed using infrared (IR) or other state-of-the-art imaging methods [13–16]. The textile-infused sensor array is built on the temperature dependence of the electrical resistance of reduced graphene oxide (rGO). We have previously exploited this behavior of rGO to produce and demonstrate conformal (>1000 mechanical bending cycles), precise (± 0.01 °C), responsive (~0.1 s), and miniaturized (10 nm thick and 50 nm wide) temperature sensing elements [17].

The conformal nature of rGO is truly unique since all other known temperature-sensing materials are ceramic-, silicon-, and metal-based. These conventional materials are rigid and brittle [18–20], and are not sufficiently conformal to be integrated into textiles at a fabric filament level. rGO is conformal because of its molecular level thickness as a 2D material. Graphene oxide (GO) is typically produced by chemical exfoliation of graphite powder [21–23]. GO consists of monolayers of carbon atoms packed into a two-dimensional (2D) honeycomb lattice [24,25] with some of the carbon atoms functionalized with oxygen-containing groups [26]. GO is a water-soluble, electrically nonconductive material. However, by thermal, chemical or photo-catalyst reduction, oxygen-containing groups can be removed and electrical conductivity can be restored to a certain extent in rGO [27,28]. We previously found [17] that rGO behaves as an NTC material, which is characterized by an exponential relationship between temperature increase and electrical resistance decrease. The NTC behavior provides an accurate mechanism of temperature sensing. In addition, rGO has found to sensitive to humidity [29,30] and pressure

* Corresponding author.
E-mail address: wlee@stevens.edu (W. Lee).

https://doi.org/10.1016/j.sna.2018.06.043
0924-4247/

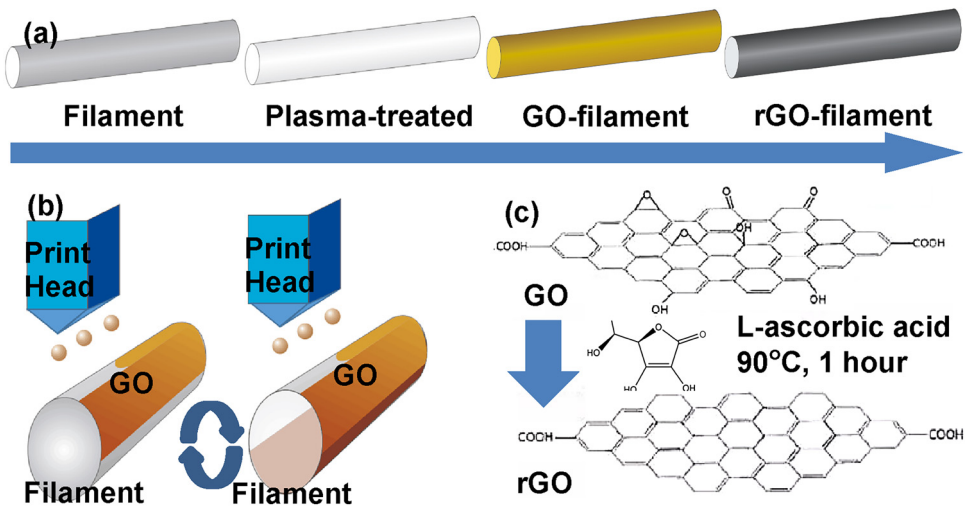

Fig. 1. Fabrication procedures of rGO-coated nylon filaments: (a) major steps, (b) inkjet printed GO on filament surface, and (c) chemical reduction of GO into rGO.

[31] and can be further functionalized for a wide variety of sensor applications [32–34].

The specific objectives of this paper were to: (1) fabricate rGO-coated nylon filaments by inkjet-printing and chemical reduction, (2) integrate rGO-coated filaments with Ag conductive threads into a polyester fabric to create an array of rGO sensing elements, (3) evaluate the conformal nature of the rGO film upon mechanical stretching and bending, and (4) evaluate the temperature-mapping attribute of the sensor array in comparison to infrared imaging.

2. Experimental

2.1. Materials

The commercial available high-purity aqueous solution of GO (2 mg/ml, purity > 99%), supplied by CheapTubes. (Brattleboro, VT, USA) with thickness of 0.7–1.2 nm and diameter of 300–800 nm, were used. The nylon filaments (>99% polyamide, diameter 500 μm) and polyester fabric (100% polyester) were purchased from Amazon. The nylon filaments provided a chemically stable and smooth substrate surface while being highly flexible and stretchable [35–37]. The polyester fabric provided excellent flexibility along with good heat conductivity and electrical insulation [38,39]. The conductive Ag threads were purchased from Syscom Advanced Materials. The conductive Cu tape, which was used as for electrodes, was purchased from R.S. Hughes.

2.2. Fabrication of rGO-coated filaments

As illustrated in Fig. 1, rGO-coated nylon filaments were produced by inkjet-printing of GO suspended in water [40–42] and subsequent chemical reduction of GO using L-ascorbic acid [25,43–45]. Nylon filaments were rinsed with deionized water and isopropyl alcohol and treated with oxygen plasma for 10 min using a plasma cleaner (Harrick Plasma) to make the filament surface hydrophilic. GO sheets were printed on nylon filaments using a Dimatrix FujiFilm inkjet printer (DMP-2831). This printer was equipped with a printhead/cartridge configuration consisting of 16 microfabricated piezoelectric nozzles with each nozzle programmable and addressable with 5 μm positioning resolution. Cartridge height and substrate temperature were maintained at 0.5 mm and 25 °C, respectively. The GO ink was printed on one side of the filaments with a cartridge that generated 10 pL ink droplets. After the GO ink was dried, the filaments were turned over to print on the other side. The printed GO was reduced using an aqueous solution of L-ascorbic acid (reagent grade, Sigma-Aldrich) at 90 °C for 1 h, and were dried at 70 °C for 12 h. The resistance of rGO on nylon was about 10 kΩ/mm whereas the resistance was higher than 100 MΩ/mm prior to chemical reduction.

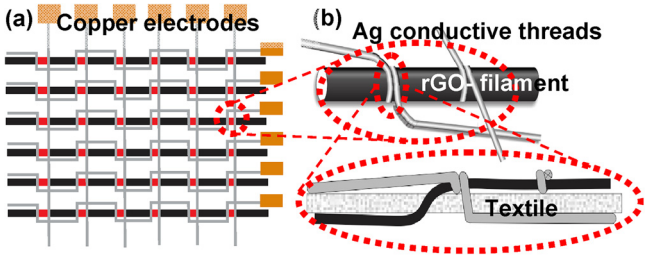

Fig. 2. Textile-infused array of 6 × 6 temperature sensors: (a) array design, (b) interfacial connection between rGO-coated filaments and conductive Ag threads.

2.3. Fabric infusion of temperature sensor array

As schematically illustrated in Fig. 2a, six rGO-coated nylon filaments and twelve Ag conductive threads were stitched into the polyester fabric to create an array consisting of 6 × 6 sensing elements. Six of the Ag threads were aligned parallel to the rGO-coated filaments with the other six threads oriented perpendicular. Fig. 2b illustrates that the electrical connections were made by looping the Ag threads tightly around the rGO-coated filaments. The length of each active sensing element was defined and controlled by producing a 1-mm distance between the perpendicular and parallel loops. The sensing elements were individually and externally read by connecting the Ag threads to conductive copper tapes attached to fabric edges. This array design was possible since the resistance of the 1-mm rGO sensing element was about 7 orders of magnitude higher than that of the Ag thread ($\sim 10^4$ vs. $\sim 10^{-3}$ Ω/mm).

2.4. Instrument and analysis

The surface morphology of rGO film was examined with scanning electron microscopy (SEM, Zeiss Auriga Small Dual-Beam FIB-SEM microscope). Captured micrographs were processed using the image processing software (ImageJ). For temperature sensitivity testing, the rGO-coated filaments were placed on a Sawatec HP-150 hot plate for temperature control. For tensile testing, the strain was measured using a Materials Testing System machine (ME-8236), and the data was processed using Pasco Capstone. The

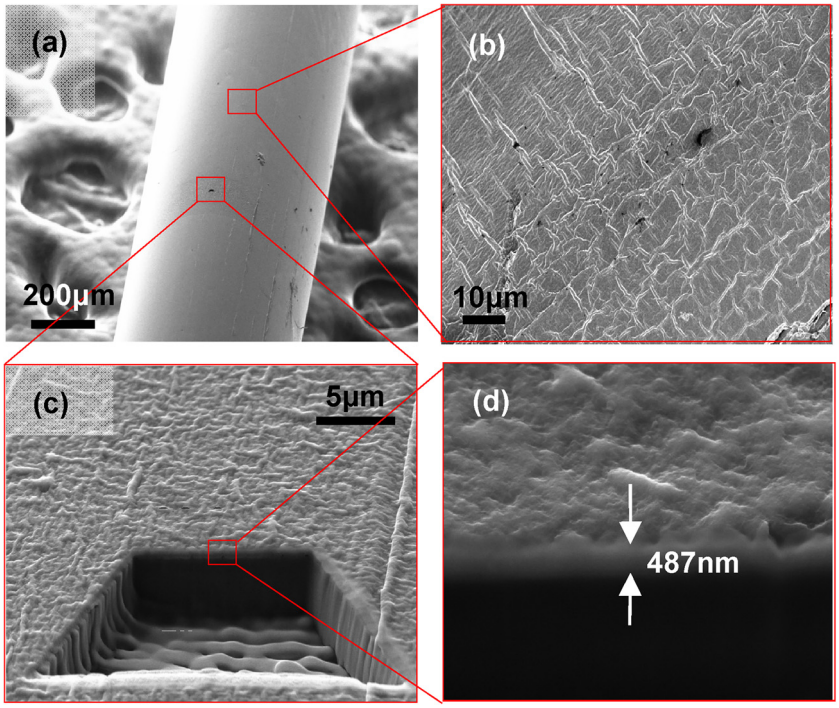

Fig. 3. rGO-coated nylon filaments: (a) and (b) surface SEM images and (c) and (d) cross-sectioned FIB/SEM view.

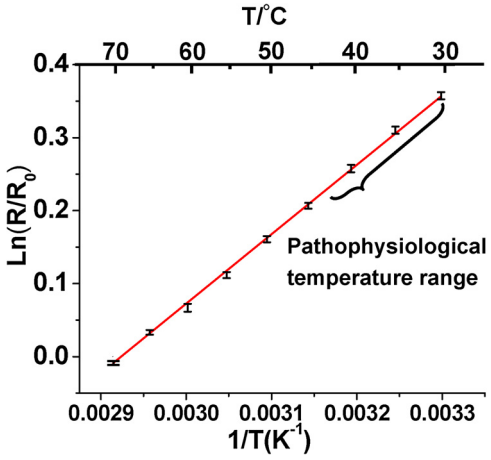

Fig. 4. Consistent NTC behavior measured from 6 sensors as indicated by low standard deviations.

resistance of rGO-coated filaments was measured using a standard 2-probe method with a Keithley 2000 multimeter.

3. Results

3.1. Morphology and conformality of rGO-coated filaments

Fig. 3a shows that the surface morphology of rGO-coated nylon filaments was uniform and continuous. Also, the cross-section images in Fig. 3c and d show that the rGO film was dense and adhered well to the filament surface. As shown in Fig. 4, the NTC behavior from six different rGO-coated filament sensors was analyzed using Eq. (1) and found to be consistent as indicated by low standard deviations:

$$R = R_0 \exp\left(\beta \frac{T_0 - T}{T_0 \bullet T}\right) \quad (1)$$

where R_0 is the initial resistance of the sensor at a reference temperature, T_0; R is the resistance at a temperature, T; and β is the temperature sensitivity parameter which is determined by fitting experimental data with the equation.

The mechanical and electrical responses of rGO-coated filament sensors under stretching and bending are shown in Figs. 5 and 6, respectively. With stretching, R/R_0 increased then sharply to 300% at 12% strain and, upon release, did not return to its original value and remained about 22.4% higher (Fig. 5a). Comparison of the SEM pictures in Fig. 5a show significant localized buckling of rGO film after the 12% strain was released. Note that we experimentally determined that nylon filaments did not plastically deform up to 20% strain. However, the resistance change was more tolerable with moderate strain. In Fig. 5b, the resistance was measured during 100 stretching cycles of 4% strain, which caused relatively small resistance changes of up to 1.76%. The changes in R/R_0 remained within 2.6% upon moderate bending up to 34° as shown in Fig. 5c. The moderate effect of bending could be explained since the 34° bending generates a tensile strain of 1.5% which is less than the observed strain limit of 4% in Fig. 5b. The rGO-coated filament was then tested in 100 34°-bending cycles, after which the resistance of rGO slightly increased by 1.92%. As can be seen in Fig. 5e, f, and g, with more severe bending to 117°, cracking was observed in the region under tension and buckling at the compressed region. Compared with cracking, buckling made more morphological damage to rGO coating, which explains why the bending testing resulted in more resistance change than tensile testing did.

3.2. Mapping capability of the temperature sensor array

As shown in Fig. 6, the textile-infused temperature sensor array was used to spatially map a human finger touching the textile. After each sensor element was calibrated at several temperatures, the temperature mapping attribute of the sensor array was evaluated by placing a finger on the fabric. Fig. 6c shows that the calibrated temperature map measured by the sensor array, highlighting the area touched by the finger with the lower resistance of the sen-

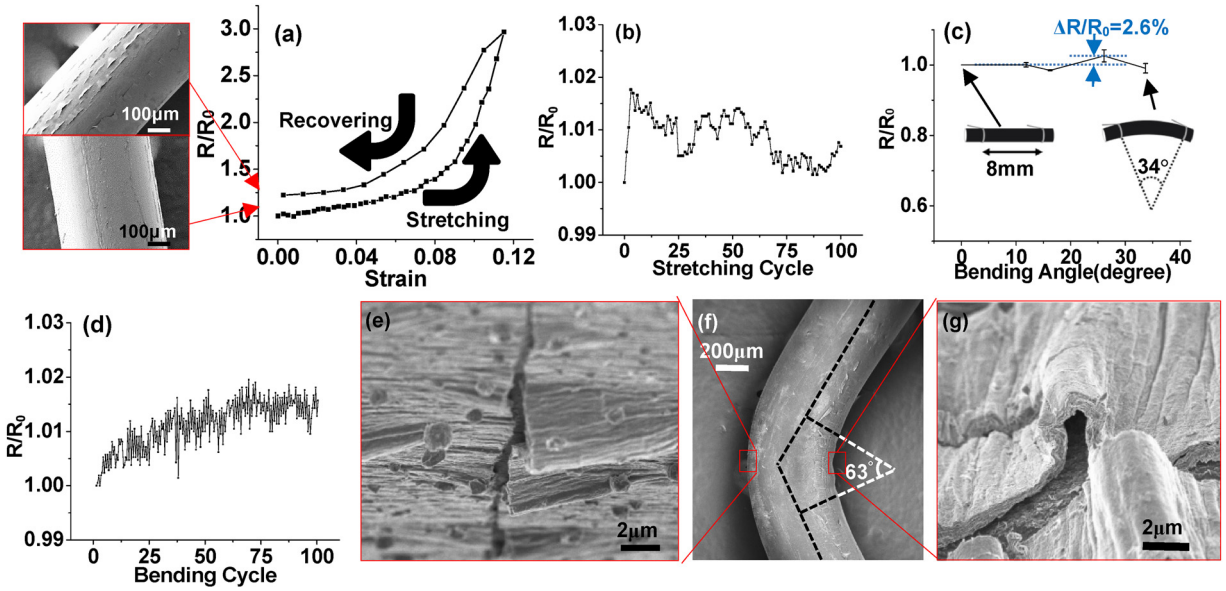

Fig. 5. Resistance change upon stretching and bending: (a) irreversible increases in R due to the cracking and buckling upon stretching up to 12% as shown by the inset SEM images before and after stretching; (b) resistance change of rGO with moderate stretching (4% strain) up to 100 stretching cycles; (c) small fluctuations in resistance of rGO with bending to 34° and (d) resistance change of rGO up to 100 34°-bending cycles. (f) SEM images of rGO-coated nylon filament after severe bending of 117° with (e) cracking at the stretched area and (g) buckling observed at the compressed region.

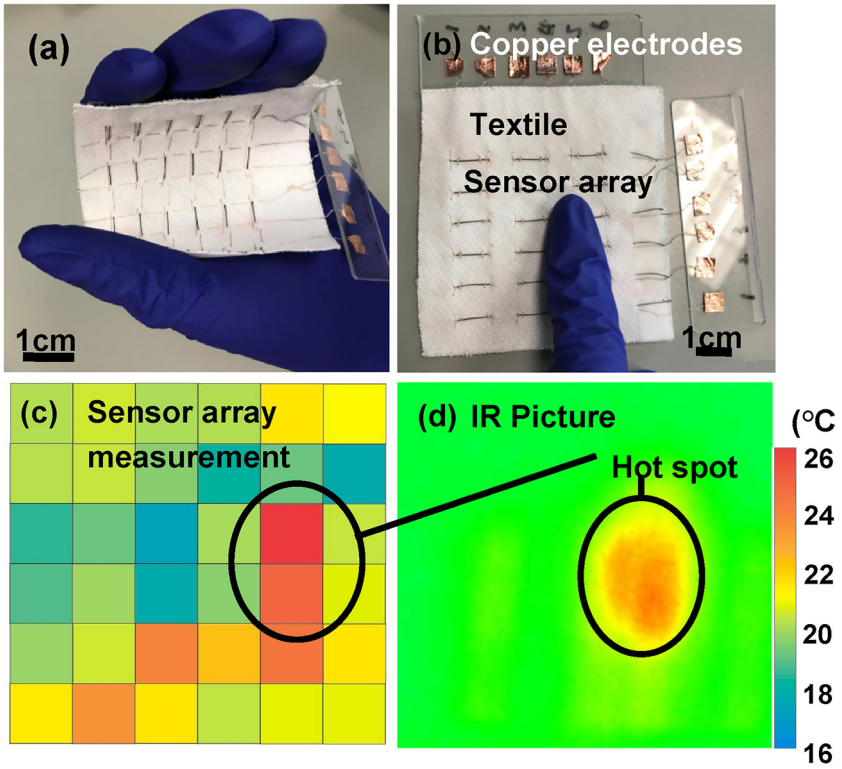

Fig. 6. (a) Optical image of the textile-infused array of 6 × 6 temperature sensors. (b) The sensor array touched by a thumb to generate the temperature distribution measured by (c) the sensor array and (d) an IR camera.

sors at the locations touched by the finger. In Fig. 6d, a thermal map of the fabric was taken using an IR camera right after touching the fabric for 1 min and then removing the finger for comparison. Based on the Fig. 6c and d, the measurements between our sensor array and the typical IR camera was determined to be within ± 2 °C. Theoretically, note that the spatial resolution of the textile-infused sensor array depends on the diameters of rGO-coated filaments and conductive threads. Based on their current diameters (0.25 mm for nylon and 0.2 mm for Ag threads), an array of 8000 sensors could be integrated into an 8 cm × 8 cm fabric piece.

4. Discussion

The results from the sensor array study provide an interesting basis to compare with other known methods of mapping skin temperatures, particularly in the context of monitoring plantar

temperatures of diabetic patients as an indicator of diabetic foot ulceration [4–7]. Current clinical standard is tactile determination and estimation of foot skin temperatures by clinicians. Two types of devices have been developed for this

application. The first category includes handheld IR cameras [46–48], which require a line of sight. The second type includes rigid thermistor- or colorimetric liquid crystal-based mats which patients step onto [49,50]. All of these devices are fundamentally limited for convenient use, and therefore are not used widely. The rGO sensors can resolve temperature differences of 0.1 °C. This sensitivity is comparable to other wearable temperature sensors reported recently [46–50]. Also, the sensitivity of rGO sensors is sufficient to spatially resolve skin temperature distributions of pathophysiological development, e.g., 5 °C variations across a 1-cm-wide ulcer [51]. The wearable configuration of our textile-infused sensor array approach provides the possibility of thermally mapping the topographically complex plantar surface in conformal, intimate, breathable, and comfortable contact. We envision that these advantages of textile-infused sensor arrays can be utilized for smart health applications, beyond monitoring diabetic foot ulceration, such as monitoring chronic wound healing, projecting ovulation cycles, detecting sleepiness and anxiety, etc.

Nevertheless, these results bring out several major challenges associated with further developments of textile-infused temperature sensors. First, it was experimentally difficult to keep consistent electrical connections between the Ag threads and rGO-coated filaments upon stretching and bending. The use of mechanically conformal and electrically conductive polymeric bonding materials, like polyaniline [52–54] and polypyrrole [55–57], could be optimized in the future. Second, our results on restorable ΔR increases as well as irreversible ΔR hysteresis above the stretching and bending suggest that the weak bonding between individual rGO sheets may be responsible for the mechanical instability of the rGO film under high strains.

The reversible changes in the NTC parameters under the moderate mechanical strains can be explained by considering that the film is an assembly of numerous rGO sheets which are held together by Van der Waals forces. The magnitude of these weak forces are highly dependent on the distance between adjacent sheets, and were therefore easily susceptible to reversible physical separations and rearrangements under moderate mechanical strains. However, with significant strains, the assembled structure would be more permanently changed via buckling and cracking mechanisms. Our result showed that the rGO sensors could be stretched up to 4% strain without significant damage remained. We viewed that this stretchability to 4% strain is quite impressive, considering all other temperature sensing materials (i.e., metals and ceramics) would not be able to withstand such strains without irreversible damage. Though our sensors were not able to avoid damage from severe tension and compression process, they could stay sensitive and reliable at some parts of bodies where the motion is moderate, like foreheads and chests. Even for the stage right now, our sensors on filaments have shown their fundamental value for physiological temperature measurement. We recognize that strain-induced variations in resistance of rGO sensors will interfere with calibrating and measuring spatiotemporal temperature distributions when fabric-infused sensor arrays dynamically deformed. This is an important issue that will potentially limit the practical use of our fabric-infused sensor array approach. One possible solution to this problem may be to covalently crosslink rGO sheets to strengthen their bonding and thus stabilize strain-induced resistance changes.

Broadly, the use of our textile-infused sensor array approach can be extended to monitor other physiological parameters since rGO is a multi-functional material which is sensitive to moisture [58], pressure [59–61], strain [62,63], and specific ions [64,65]. From a fabrication perspective, the combinative use of inkjet printing and chemical reduction provides an important capability to precisely deposit rGO on the filament surface with ~50 μm spatial resolution in the lateral direction and ~20 nm thick [28,42]. This fabrication approach offers the possibility of additive, net-shape manufacturing with minimum use and waste generation of GO. Also, the approach would be easily integrated into standard roll-to-roll textile filament manufacturing using commercial inkjet print-heads for high-volume and thus low-cost production of smart fabrics.

5. Conclusions

We designed and fabricated the textile-infused sensor array, utilizing rGO as a uniquely conformal NTC material, for spatiotemporal mapping of skin temperatures. The rGO-coated nylon filaments were produced by inkjet-printing and chemical reduction. Moderate bending (<34°) and stretching (<4% strain) did not cause appreciable and irreversible resistance change of rGO film, and therefore the stable NTC behavior could be sustained. The rGO-coated nylon filaments were stitched along with Ag conductive threads into a polyester fabric to create the array, consisting of individually addressable 6 × 6 NTC sensing elements. The temperature-mapping attribute of the sensor array was evaluated in comparison to infrared imaging.

Acknowledgments

We are grateful for the SEM characterization support from Dr. Alex Chou. Research in this publication was supported in part by the grant from the National Science Foundation (SBIR 1648057).

References

[1] S.A. Carter, R.B. Tate, The effect of body heating and cooling on the ankle and toe systolic pressures in arterial disease, J. Vasc. Surg. 16 (1992) 148–153, http://dx.doi.org/10.1016/0741-5214(92)90102-E.
[2] R.F. Gillum, Body temperature and its relationship to demographic and cardiovascular risk factors in a national sample of children and adolescents, J. Natl. Med. Assoc. 84 (1992) 591–599.
[3] S. Bhutani, T.J.R. Francis, A.J. Young, D.A. Stulz, S.R. Muza, J.W. Castellani, et al., Cardiovascular function in heat-stressed human, J. Appl. Physiol. 84 (2000) 52–69, http://dx.doi.org/10.1111/j.1748-1716.2010.02119.x.Cardiovascular.
[4] S. Bagavathiappan, J. Philip, T. Jayakumar, B. Raj, P.N.S. Rao, M. Varalakshmi, V. Mohan, Correlation between plantar foot temperature and diabetic neuropathy: a case study by using an infrared thermal imaging technique, J. Diabetes Sci. Technol. 4 (2010) 1386–1392, http://dx.doi.org/10.1177/193229681000400613.
[5] A. Skafjeld, M.M. Iversen, I. Holme, L. Ribu, K. Hvaal, B.K. Kilhovd, A pilot study testing the feasibility of skin temperature monitoring to reduce recurrent foot ulcers in patients with diabetes - a randomized controlled trial, BMC Endocr. Disord. 15 (2015) 55, http://dx.doi.org/10.1186/s12902-015-0054-x.
[6] P.C. Sun, H. Da Lin, S.H.E. Jao, Y.C. Ku, R.C. Chan, C.K. Cheng, Relationship of skin temperature to sympathetic dysfunction in diabetic at-risk feet, Diabetes Res. Clin. Pract. 73 (2006) 41–46, http://dx.doi.org/10.1016/j.diabres.2005.12.012.
[7] V.J. Houghton, V.M. Bower, D.C. Chant, Is an increase in skin temperature predictive of neuropathic foot ulceration in people with diabetes? A systematic review and meta-analysis, J. Foot Ankle Res. 6 (2013) 1–13, http://dx.doi.org/10.1186/1757-1146-6-31.
[8] L. Nummenmaa, E. Glerean, R. Hari, J.K. Hietanen, Bodily maps of emotions, Proc. Natl. Acad. Sci. U. S. A. 111 (2014) 646–651, http://dx.doi.org/10.1073/pnas.1321664111.
[9] L.M. Castano, A.B. Flatau, Smart fabric sensors and e-textile technologies: a review, Smart Mater. Struct. 23 (2014) 53001, http://dx.doi.org/10.1088/0964-1726/23/5/053001.
[10] K. Cherenack, L. Van Pieterson, Smart textiles: challenges and opportunities, J. Appl. Phys. 112 (2012), http://dx.doi.org/10.1063/1.4742728.
[11] D. Meoli, T. May-plumlee, Interactive electronic textile development: a revew of technologies, J. Text. Appar. Technol. Manag. 2 (2002) 1–12.
[12] B.S. Shim, W. Chen, C. Doty, C. Xu, N.A. Kotov, Smart electronic yarns and wearable fabrics for human biomonitoring made by carbon nanotube coating with polyelectrolytes, Nano Lett. 8 (2008) 4151–4157, http://dx.doi.org/10.1021/nl801495p.
[13] N. Ludwig, D. Formenti, M. Gargano, G. Alberti, Skin temperature evaluation by infrared thermography: comparison of image analysis methods, Infrared Phys. Technol. 62 (2014) 1–6, http://dx.doi.org/10.1016/j.infrared.2013.09.011.

[14] M.S.V. Salles, S.C. da Silva, F.A. Salles, L.C. Roma, L. El Faro, P.A. Bustos Mac Lean, C.E. Lins de Oliveira, L.S. Martello, Mapping the body surface temperature of cattle by infrared thermography, J. Therm. Biol. 62 (2016) 63–69, http://dx.doi.org/10.1016/j.jtherbio.2016.10.003.
[15] S. Harada, W. Honda, T. Arie, S. Akita, K. Takei, Fully printed, highly sensitive multifunctional artificial electronic whisker arrays integrated with strain and temperature sensors, ACS Nano 8 (2014) 3921–3927, http://dx.doi.org/10.1021/nn500845a.
[16] L. Gao, Y. Zhang, V. Malyarchuk, L. Jia, K.-I. Jang, R.C. Webb, H. Fu, Y. Shi, G. Zhou, L. Shi, D. Shah, X. Huang, B. Xu, C. Yu, Y. Huang, J.A. Rogers, Epidermal photonic devices for quantitative imaging of temperature and thermal transport characteristics of the skin, Nat. Commun. 5 (2014) 4938, http://dx.doi.org/10.1038/ncomms5938.
[17] D. Kong, L.T. Le, Y. Li, J.L. Zunino, W. Lee, Temperature-dependent electrical properties of graphene inkjet-printed on flexible materials, Langmuir 28 (2012) 13467–13472, http://dx.doi.org/10.1021/la301775d.
[18] D.H. Ho, Q. Sun, S.Y. Kim, J.T. Han, D.H. Kim, J.H. Cho, Stretchable and multimodal all graphene electronic skin, Adv. Mater. 28 (2016) 2601–2608, http://dx.doi.org/10.1002/adma.201505739.
[19] A. Feteira, Negative temperature coefficient resistance (NTCR) ceramic thermistors: an industrial perspective, J. Am. Ceram. Soc. 92 (2009) 967–983, http://dx.doi.org/10.1111/j.1551-2916.2009.02990.x.
[20] A. Rousset, R. Legros, A. Lagrange, Recent progress in the fabrication of ceramic negative temperature coefficient thermistors, J. Eur. Ceram. Soc. 13 (1994) 185–195, http://dx.doi.org/10.1016/0955-2219(94)90027-2.
[21] C. Botas, P. Álvarez, P. Blanco, M. Granda, C. Blanco, R. Santamaría, L.J. Romasanta, R. Verdejo, M.A. López-Manchado, R. Menéndez, Graphene materials with different structures prepared from the same graphite by the Hummers and Brodie methods, Carbon N. Y. 65 (2013) 156–164, http://dx.doi.org/10.1016/j.carbon.2013.08.009.
[22] J. Chen, B. Yao, C. Li, G. Shi, An improved Hummers method for eco-friendly synthesis of graphene oxide, Carbon N. Y. 64 (2013) 225–229, http://dx.doi.org/10.1016/j.carbon.2013.07.055.
[23] J. Chen, Y. Li, L. Huang, C. Li, G. Shi, High-yield preparation of graphene oxide from small graphite flakes via an improved Hummers method with a simple purification process, Carbon N. Y. 81 (2015) 826–834, http://dx.doi.org/10.1016/j.carbon.2014.10.033.
[24] A.K. Geim, Graphene: status and prospects, Science (80-.) 324 (2012) 1530–1534, http://dx.doi.org/10.1126/science.1158877.
[25] K.S. Novoselov, D. Jiang, F. Schedin, T.J. Booth, V.V. Khotkevich, S.V. Morozov, A.K. Geim, Two-dimensional atomic crystals, Proc. Natl. Acad. Sci. 102 (2005) 10451–10453, http://dx.doi.org/10.1073/pnas.0502848102.
[26] R.S. Ruoff, DaneilR. Dreyer, Sungjin Park, Christopher W. Bielawski, The chemistry of graphene oxide, graphene oxide reduct. Recipes, Spectrosc. Appl. (2015) 61–95, http://dx.doi.org/10.1007/978-3-319-15500-5_3.
[27] R. Kazemzadeh, K. Andersen, L. Motha, W.S. Kim, Photother. Reduced Graphene Oxide 36 (2015) 180–182.
[28] K.K. Sadasivuni, A. Kafy, H.-C. Kim, H.-U. Ko, S. Mun, J. Kim, Reduced graphene oxide filled cellulose films for flexible temperature sensor application, Synth. Met. 206 (2015) 154–161, http://dx.doi.org/10.1016/j.synthmet.2015.05.018.
[29] D. Zhang, J. Tong, B. Xia, Humidity-sensing properties of chemically reduced graphene oxide/polymer nanocomposite film sensor based on layer-by-layer nano self-assembly, Sensors Actuators B Chem. 197 (2014) 66–72, http://dx.doi.org/10.1016/j.snb.2014.02.078.
[30] D. Toloman, A. Popa, M. Stan, C. Socaci, A.R. Biris, G. Katona, F. Tudorache, I. Petrila, F. Iacomi, Reduced graphene oxide decorated with Fe doped SnO2 nanoparticles for humidity sensor, Appl. Surf. Sci. 402 (2017) 410–417, http://dx.doi.org/10.1016/j.apsusc.2017.01.064.
[31] Z. Lou, S. Chen, L. Wang, K. Jiang, G. Shen, An ultra-sensitive and rapid response speed graphene pressure sensors for electronic skin and health monitoring, Nano Energy 23 (2016) 7–14, http://dx.doi.org/10.1016/j.nanoen.2016.02.053.
[32] Y. Zhou, Y. Jiang, G. Xie, Gas sensors for CO2 detection based on RGO – PEI films at room temperature, Chin. Sci. Bull. 59 (2014) 1999–2005, http://dx.doi.org/10.1007/s11434-014-0253-2.
[33] Q. Feng, X. Li, J. Wang, A.M. Gaskov, Reduced graphene oxide (rGO) encapsulated Co3O4 composite nanofibers for highly selective ammonia sensors, Sens. Actuators B Chem. 222 (2016) 864–870, http://dx.doi.org/10.1016/j.snb.2015.09.021.
[34] B. Sun, K. Zhang, L. Chen, L. Guo, S. Ai, A novel photoelectrochemical sensor based on PPIX-functionalized WO3-rGO nanohybrid-decorated ITO electrode for detecting cysteine, Biosens. Bioelectron. 44 (2013) 1–4, http://dx.doi.org/10.1016/j.bios.2013.01.014.
[35] T. Kawaguchi, The dynamic mechanical properties, J. Appl. Polym. Sci. 1 (1959) 56–61.
[36] H. Search, C. Journals, A. Contact, M. Iopscience, I.P. Address, Energetically Stable Conformations of Nylon 66 and Nylon 6 Molecules in Crystals, 4474 (n.d.).
[37] M.L. Tate, Y.K. Kamath, S.P. Wesson, S.B. Ruetsch, Surface energetics of nylon 66 fibers, J. Colloid Interface Sci. 177 (1996) 579–588, http://dx.doi.org/10.1006/jcis.1996.0072.
[38] R.A. Cass, Unsaturated polyesters. Structure and properties, J. Am. Chem. Soc. 87 (1965), http://dx.doi.org/10.1021/ja01088a051, 2304–2304.
[39] W.O. Baker, W.A. Yager, The relation of dielectric properties to structure of crystalline polymers. II. Linear polyamides, J. Am. Chem. Soc. 64 (1942) 2171–2177, http://dx.doi.org/10.1021/ja01261a043.
[40] L.T. Le, M.H. Ervin, H. Qiu, B.E. Fuchs, J. Zunino, W.Y. Lee, Inkjet-printed graphene for flexible micro-supercapacitors, Proc. IEEE Conf. Nanotechnol. (2011) 67–71, http://dx.doi.org/10.1109/NANO.2011.6144432.
[41] M.H. Ervin, L.T. Le, W.Y. Lee, Inkjet-printed flexible graphene-based supercapacitor, Electrochim. Acta 147 (2014) 610–616, http://dx.doi.org/10.1016/j.electacta.2014.10.006.
[42] L.T. Le, M.H. Ervin, H. Qiu, B.E. Fuchs, W.Y. Lee, Graphene supercapacitor electrodes fabricated by inkjet printing and thermal reduction of graphene oxide, Electrochem. Commun. 13 (2011) 355–358, http://dx.doi.org/10.1016/j.elecom.2011.01.023.
[43] A. Abulizi, K. Okitsu, J.J. Zhu, Ultrasound assisted reduction of graphene oxide to graphene in l-ascorbic acid aqueous solutions: kinetics and effects of various factors on the rate of graphene formation, Ultrason. Sonochem. 21 (2014) 1174–1181, http://dx.doi.org/10.1016/j.ultsonch.2013.10.019.
[44] X. Zhu, Q. Liu, X. Zhu, C. Li, M. Xu, Y. Liang, Reduction of graphene oxide via ascorbic acid and its application for simultaneous detection of dopamine and ascorbic acid, Int. J. Electrochem. Sci. 7 (2012) 5172–5184.
[45] S. Uhm, N.H. Tuyen, J. Lee, Controlling oxygen functional species of graphene oxide for an electro-oxidation of L-ascorbic acid, Electrochem. Commun. 13 (2011) 677–680, http://dx.doi.org/10.1016/j.elecom.2011.04.006.
[46] B.B. Lahiri, S. Bagavathiappan, T. Jayakumar, J. Philip, Medical applications of infrared thermography: a review, Infrared Phys. Technol. 55 (2012) 221–235, http://dx.doi.org/10.1016/j.infrared.2012.03.007.
[47] A. Rogalski, Infrared detectors: an overview, Infrared Phys. Technol. 43 (2002) 187–210, http://dx.doi.org/10.1016/S1350-4495(02)00140-8.
[48] V. Bernard, E. Staffa, V. Mornstein, A. Bourek, Infrared camera assessment of skin surface temperature - effect of emissivity, Phys. Med. 29 (2013) 583–591, http://dx.doi.org/10.1016/j.ejmp.2012.09.003.
[49] D.-I. Kim, T. Quang Trung, B.-U. Hwang, J.-S. Kim, S. Jeon, J. Bae, J.-J. Park, N.-E. Lee, A sensor array using multi-functional field-effect transistors with ultrahigh sensitivity and precision for bio-monitoring, Sci. Rep. 5 (2015) 12705, http://dx.doi.org/10.1038/srep12705.
[50] T. Vuorinen, J. Niittynen, T. Kankkunen, T.M. Kraft, M. Mäntysalo, Inkjet-printed graphene/PEDOT:PSS temperature sensors on a skin-conformable polyurethane substrate, Sci. Rep. 6 (2016) 35289, http://dx.doi.org/10.1038/srep35289.
[51] T. Kanazawa, A. Kitamura, G. Nakagami, T. Goto, T. Miyagaki, A. Hayashi, S. Sasaki, Y. Mugita, S. Iizaka, H. Sanada, Lower temperature at the wound edge detected by thermography predicts undermining development in pressure ulcers: a pilot study, Int. Wound J. 13 (2015) 454–460.
[52] A.G. MacDiarmid, "Synthetic metals": a novel role for organic polymers (nobel lecture), Angew. Chem. Int. Ed. 40 (2001) 2581–2590, http://dx.doi.org/10.1002/1521-3773(20010716)40:14<2581::AID-ANIE2581>3.0.CO;2-2.
[53] A.G. Macdiarmid, J.C. Chiang, A.F. Richter, A.J. Epstein, Polyaniline: a new concept in conducting polymers, Synth. Met. 18 (1987) 285–290, http://dx.doi.org/10.1016/0379-6779(87)90893-9.
[54] W.-S. Huang, B.D. Humphrey, A.G. MacDiarmid, Polyaniline, a novel conducting polymer. Morphology and chemistry of its oxidation and reduction in aqueous electrolytes, J. Chem. Soc. Faraday Trans. 1 Phys. Chem. Condens. Phases 82 (1986) 2385, http://dx.doi.org/10.1039/f19868202385.
[55] T. Vernitskaya, O. Efimov, Polypyrrole: a conducting polymer; Its synthesis, properties and applications, Russ. Chem. Rev. (1997) http://www.turpion.org/php/paper.phtml?journal_id=rc&paper_id=261.
[56] E.M. Genies, G. Bidan, a.F. Diaz, Spectroelectrochemical study of polypyrrole films, J. Electroanal. Chem. Interfacial Electrochem. 149 (1983) 101–113, http://dx.doi.org/10.1016/S0022-0728(83)80561-0.
[57] W. Li, Q. Zhang, G. Zheng, Z.W. Seh, H. Yao, Y. Cui, Understanding the role of different conductive polymers in improving the nanostructured sulfur cathode performance, Nano Lett. 13 (2013) 5534–5540, http://dx.doi.org/10.1021/nl403130h.
[58] S. Borini, R. White, D. Wei, M. Astley, S. Haque, E. Spigone, N. Harris, J. Kivioja, T. Ryhänen, Ultrafast graphene oxide humidity sensors, ACS Nano 7 (2013) 11166–11173, http://dx.doi.org/10.1021/nn404889b.
[59] H. Bin Yao, J. Ge, C.F. Wang, X. Wang, W. Hu, Z.J. Zheng, Y. Ni, S.H. Yu, A flexible and highly pressure-sensitive graphene-polyurethane sponge based on fractured microstructure design, Adv. Mater. 25 (2013) 6692–6698, http://dx.doi.org/10.1002/adma.201303041.
[60] H. Tian, Y. Shu, X.-F. Wang, M.A. Mohammad, Z. Bie, Q.-Y. Xie, C. Li, W.-T. Mi, Y. Yang, T.-L. Ren, A graphene-based resistive pressure sensor with record-high sensitivity in a wide pressure range, Sci. Rep. 5 (2015) 8603, http://dx.doi.org/10.1038/srep08603.
[61] S. Chun, Y. Kim, H. Jin, E. Choi, S.B. Lee, W. Park, A graphene force sensor with pressure-amplifying structure, Carbon N. Y. 78 (2014) 601–608, http://dx.doi.org/10.1016/j.carbon.2014.07.051.
[62] J. Zhao, G.-Y. Zhang, D.-X. Shi, Review of graphene-based strain sensors, Chin. Phys. B 22 (2013) 57701, http://dx.doi.org/10.1088/1674-1056/22/5/057701.
[63] X. Li, R. Zhang, W. Yu, K. Wang, J. Wei, D. Wu, A. Cao, Z. Li, Y. Cheng, Q. Zheng, R.S. Ruoff, H. Zhu, Stretchable and highly sensitive graphene-on-polymer strain sensors, Sci. Rep. 2 (2012) 1–6, http://dx.doi.org/10.1038/srep00870.
[64] J. Li, L. Lu, T. Kang, S. Cheng, Intense charge transfer surface based on graphene and thymine-Hg(II)-thymine base pairs for detection of Hg2+, Biosens. Bioelectron. 77 (2016) 740–745, http://dx.doi.org/10.1016/j.bios.2015.10.047.
[65] F. Tan, L. Cong, X. Jiang, Y. Wang, X. Quan, J. Chen, A. Mulchandani, Highly sensitive detection of Cr(VI) by reduced graphene oxide chemiresistor and 1,4-dithiothreitol functionalized Au nanoparticles, Sens. Actuators B Chem. 247 (2017) 265–272, http://dx.doi.org/10.1016/j.snb.2017.02.163.

Biographies

Yiqian Jin I graduated from Peking University as a bachelor of engineering in 2014. Then I came to Stevens Institute of Technology in August 2014, and graduated as a master of engineering in December 2015. Now I am working in Prof. Lee's lab as a Ph.D student. I started learning science research skills in 2011. The research I have done includes lithium ion batteries, polymers, nanospheres and graphene. Now I am focusing on the functionalization and crosslinking on graphene oxide in order to modify its sensing capability.

Eric P. Boon I am a Ph.D. graduated from Stevens Institute of Technology in 2017. I am a materials scientist with broad training in physics, synthetic chemistry and materials science. My research experience has driven my interest in carbon materials and their use as flexible printed sensors and I'm looking to help translate these exciting possibilities to commercial applications.

Linh T. Le I joined Prof. Woo Lee's lab in Fall 2009 after receiving MSc in Chemical Engineering from Columbia University and BSc in Analytical Chemistry from Vietnam National University. My research overlapped between graphene-based nanomaterial, scalable printing technology with main applications in flexible electronics. Most recently, I was interested in entrepreneurship and had co-founded a startup company, FlexTraPower to further develop the graphene technology as a commercial product.

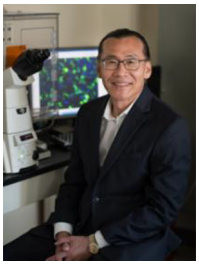

Prof. Woo Lee I joined Stevens in 1997 as Associate Professor after working at United Technologies Research Center (1990–1992) and Oak Ridge National Laboratory (1992–1997). eceived tenure in 2000, and was promoted to Professor in 2001. From 2000 to 2005, I chaired the Department of Chemical, Biomedical and Materials Engineering. During this period, the Department's annual research expenditures increased from $1M to $2.2M. Under my administrative leadership, the Biomedical Engineering program was launched in 2002. I was awarded with Stevens' honorary Master of Engineering degree in 2008 for my service to the Institute. My latest passion is to explore the possibility of developing microfluidic tissue models, as an entirely new way of studying how human tissues interact with drugs, pathogens, and biomaterials. I believe this new approach is expected to: (1) reduce reliance on animal studies since they do not often predict human response and (2) provide a path for the potential development of assays to assist in therapeutic decision-making. Also, I have been fascinated by graphene as a truly flexible, potentially low-cost material that wrinkles and folds at a nanoscale while being mechanically strong and electrochemically inert.